

# JOURNAL OF THE AMERICAN CHEMICAL SOCIETY

Registered in U.S. Patent Office. © Copyright, 1979, by the American Chemical Society

VOLUME 101, NUMBER 7

MARCH 28, 1979

## Electron Nuclear Double Resonance from High- and Low-Spin Ferric Hemoglobins and Myoglobins

C. F. Mulks,<sup>1a,2</sup> C. P. Scholes,<sup>\*1a</sup> L. C. Dickinson,<sup>1b</sup> and A. Lapidot<sup>1c</sup>

*Contribution from the Department of Physics and Center for Biological Macromolecules, State University of New York at Albany, Albany, New York 12222, the Department of Chemistry, University of Massachusetts, Amherst, Massachusetts 02002, and the Isotope Department, Weizmann Institute of Science, Rehovot, Israel. Received August 28, 1978*

**Abstract:** In aquo, fluoride, azide, and cyanide derivatives of ferric hemoglobin and myoglobin, ENDOR signals have been observed and assigned. Hyperfine coupling constants have been obtained for axial ligand nuclei and for nitrogens and protons of the heme group. In aquo derivatives, but not fluoride, we have observed hyperfine couplings of about 6 MHz to exchangeable, heme-bound water protons. In both aquo and fluoride derivatives we have assigned nonexchangeable proton resonances to heme meso protons, and another exchangeable proton resonance has been assigned to the proton on the  $\delta$  nitrogen of the proximal histidine. Small changes occur in ENDOR frequencies of these latter two types of protons on going from aquo to fluoride derivatives.  $^{13}\text{C}$  couplings of  $28.64 \pm 0.08$  (myoglobin) and  $27.33 \pm 0.18$  MHz (hemoglobin) were found for heme-bound  $^{13}\text{CN}^-$ . The hyperfine couplings to heme meso protons of the cyanide derivatives decrease in the order protohemin, hemoglobin, myoglobin. In myoglobin and hemoglobin cyanide an exchangeable proton occurs that we estimate at 4.5–5.5 Å distance from the iron. Nitrogen ENDOR seen in hemoglobin and myoglobin cyanide was assigned to heme nitrogens by comparison with the nitrogen ENDOR from hemoglobin that contained  $^{15}\text{N}$  in 50% enrichment only on the heme. Differences which were particularly large in the heme plane were noted between hemoglobin and myoglobin azides. The majority of the nitrogen ENDOR features from azide complexes were assigned to heme nitrogens. As measured at the  $g$ -value extremum normal to the heme plane in myoglobin and hemoglobin azides, we found  $^{15}\text{N}$  heme hyperfine couplings in the 7.0–8.5-MHz range,  $^{14}\text{N}$  heme hyperfine couplings in the 5.0–6.5-MHz range, and first-order heme  $^{14}\text{N}$  quadrupole couplings in the 0.4–0.6-MHz range. At the  $g$ -value extremum ( $g_x$ ) in the heme plane,  $^{15}\text{N}$  heme hyperfine couplings were in the 6.0–7.5-MHz range. We have also observed ENDOR from the nitrogens of carp hemoglobin azides, which exist in the R conformation at high pH and the T conformation at low pH. Changes in electronic  $g$  values have been seen between the two forms, but we have seen no change in the heme nitrogen ENDOR between the two forms.

### Introduction

The technique of electron nuclear double resonance (ENDOR) has previously been used to probe electron–nuclear interactions in a number of heme proteins and hemin systems.<sup>3</sup> The ENDOR data serve the following purposes: (1) to provide experimental information to those who calculate heme wave functions;<sup>4</sup> (2) to provide empirical evidence on how various aspects of the heme electronic environment change in response to specific changes such as the change of one axial ligand;<sup>3d,e</sup> (3) to provide evidence for electronic changes at the heme brought on by conformational protein change.<sup>3c</sup>

The initial ENDOR work in Feher's laboratory<sup>3a-c</sup> gave heme and proximal histidine nitrogen ENDOR as well as  $^{57}\text{Fe}$  ENDOR<sup>3b</sup> from high-spin ferric aquometmyoglobin and hemoglobin. Proton ENDOR was seen from weakly coupled protons of myoglobin, although assignments to specific protons were tentative.<sup>3c</sup> In work on the naturally occurring valency hybrid, hemoglobin  $M_{\text{Milwaukee}}$ , which has normal ferrous  $\alpha$  chains but mutant ferric  $\beta$  chains, a change in the ENDOR frequencies from the proximal histidine nitrogens of the  $\beta$

chains was seen in response to the  $\text{O}_2$  or  $\text{CO}$  liganding of the normal  $\alpha$  chains.<sup>3c</sup>

More recently in work on high-spin ferric hemin systems we have definitively assigned proton ENDOR to heme meso protons and have noted variation of meso proton and heme nitrogen hyperfine couplings as a function of systematic change of hemin axial ligands.<sup>3d,e</sup> We have reported preliminary work on nitrogen and proton ENDOR in several low-spin ferric heme proteins such as cytochrome  $c$  and metmyoglobin cyanide.<sup>3f</sup> Nitrogen ENDOR was seen from these low-spin compounds, but it was not clear whether it was from heme or histidine nitrogen; proton ENDOR was also seen and two of the prominent spectral features were assigned to meso protons.<sup>3f</sup>

In this present work we have extended our ENDOR studies to heme compounds not previously looked at, such as the azide compounds of myoglobin and hemoglobin. We have seen and assigned ENDOR from heme axial ligands not previously studied, such as  $^{13}\text{CN}^-$  and the protons of heme-bound  $\text{H}_2\text{O}$ . We have studied nuclei previously seen but not assigned, such as nitrogens in cyano compounds and various weakly coupled

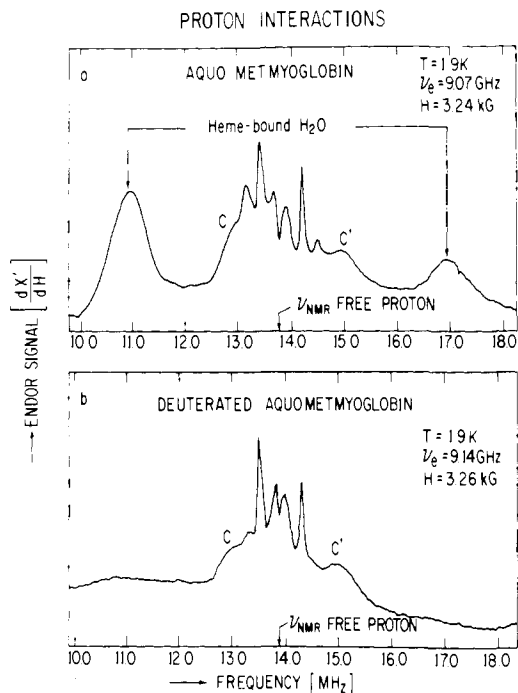


**Figure 1.** ENDOR from aquometmyoglobin in protonated (a) and deuterated solvent (b). Spectra were taken at the  $g_z = 2.00$  extremum where the magnetic field is along the heme normal. The purpose of these measurements was to show exchangeable heme-bound water protons. Although the solvent system for these spectra contained glycerol, control experiments were also run on samples without glycerol that showed that the exchangeable, heme-bound  $H_2O$  was still present. The experimental conditions are given in the Experimental Section. Each spectrum took about 45 min of signal averaging.

protons in aquo and fluoro compounds. We have looked for variation in ENDOR frequencies between hemoglobin and myoglobin compounds where the axial ligand is kept constant since we then expect that the source of such variation lies in the different environment of the heme in the two proteins.

It has been our intent to obtain in this work characteristic spectra at  $g$ -value extrema of frozen solutions. We have then attempted to assign these spectra to particular nuclei, and, if possible, have computed explicit hyperfine couplings for the nuclei studied. The present study is intended to lay the groundwork for future studies in at least three different directions: (1) complete orientation studies of single crystals to obtain the complete hyperfine tensors; (2) model studies on low-spin heme compounds to determine the factors which affect the measured hyperfine couplings; (3) studies of the effect of conformational change upon heme electronic structure. With respect to this latter goal, we have in this present work looked at carp hemoglobins which switch from the low-affinity T form to the high-affinity R form on going from low pH (4.8) to high pH (8.0).<sup>5</sup> Change in the EPR spectra of carp hemoglobin azides had previously been seen upon going from low to high pH and was interpreted as primarily coming from a change in the tetragonal component of the ligand field at the heme iron.<sup>6</sup> We wanted to see if there was an accompanying change in the underlying electronic densities seen by ENDOR.

#### Experimental Section

**Apparatus.** The ENDOR apparatus has been previously described.<sup>3,7</sup> The EPR-ENDOR cavity used here resonated in the 9.1–9.2-GHz range when loaded with sample. All ENDOR except on nitrogens of high-spin ferric heme proteins was done with the dispersion ( $\chi'$ ) EPR mode under rapid passage conditions. For bringing in weakly coupled protons with best resolution, it was desirable to use

a 100-kHz field modulation amplitude of about 0.3 G ptp (peak to peak) while a magnetic field modulation of about 1.5 G ptp was appropriate for bringing in more strongly coupled protons and all other nuclei.

**Reagents.** All common salts were Fisher ACS certified reagents or their equivalent.  $D_2O$  for deuteration experiments was purchased in 99.8% purity from Merck or from Bio-Rad. Isotopically labeled salts ( $^{13}C$ N, 90% enrichment;  $^{15}N$ NN $^-$ , 90% enrichment;  $C^{15}N^-$ , 90% enrichment) were purchased from Stohler Chemical Co. Deuterated glycerol was prepared by diluting glycerol with  $D_2O$  and vacuum distilling away the  $D_2O$  several times until the final product was about 95% deuterated in exchangeable protons. Myoglobin was Sigma type 11 sperm whale metmyoglobin. Freshly drawn human blood samples were obtained from the Hematology Department at Albany Medical Center Hospital.

**Sample Preparation.** The metmyoglobin was chromatographed on DE 52 as described previously.<sup>3a</sup> Human hemoglobin samples were prepared from red blood cells at 4 °C by the method of Drabkin.<sup>8</sup> The hemoglobin was converted to methemoglobin by addition (at room temperature) of a slight molar excess relative to heme of potassium ferricyanide. The ferricyanide was removed by chromatography on Sephadex G-25 (coarse) equilibrated with 0.1 M phosphate buffer, pH 6.8. The hemoglobin samples were concentrated by use of a Schleicher and Schuell collodion bag apparatus. Myoglobin samples were concentrated with an Amicon filtration device.

Carp hemoglobin was prepared at University of Massachusetts, Amherst, using methods detailed in ref 6. For purposes of assigning nitrogen ENDOR to heme or to histidine nitrogens, a hemoglobin enriched to 50% in  $^{15}N$  on the heme was prepared at the Isotope Department, Weizmann Institute, Rehovot, Israel. This hemoglobin was made by  $Me_2SO$ -treated Friend leukemic cells grown in cell cultures enriched with  $^{15}N$  glycine.<sup>9</sup>

The  $^{15}N$  labeling of the heme group was determined by mass spectrometric analysis of protoporphyrin IX dimethyl ester prepared from the  $^{15}N$ -labeled hemoglobin. The amino acid  $^{15}N$  labeling profile of the globin was determined by gas chromatographic-mass spectrometric analysis of the trifluoroacetyl-*n*-butyl ester derivatives of the globin hydrolysate. An enrichment in  $^{15}N$  of about 50% on the heme was found, and  $^{15}N$  on the glycine was found without significant scrambling of  $^{15}N$  with other amino acids.

Samples of 1–1.5-mL volume were frozen in 7-mm i.d. tubes by plunging into liquid nitrogen. Samples were typically 5 mM in heme and were 0.05 M in phosphate, pH 6.8. Approximately a twofold molar excess of cyanide or azide was used to convert the heme proteins to cyanide or azide derivatives. The fluoride derivatives were 0.1 M in potassium fluoride. Such a high fluoride concentration is needed to ensure ligation of heme with fluoride ion. (Because such a high fluoride concentration will significantly alter the ionic strength, we also did control experiments with 0.01 and 0.5 M fluoride.) Prior to making samples with these anions we had run titration studies in order to determine the minimum concentrations of anions necessary for saturation of the heme group with anion.

We used a 1:1 glycerol-buffer solution in making many of our samples because we had previously found that addition of glycerol often enhances the ENDOR signal (as a percentage of the EPR signal) in frozen solutions. We believe that this happens because the glycerol promotes formation of a glass and prevents the aggregation of metalloprotein upon freezing. (When paramagnetic centers aggregate, spin-spin relaxation occurs between electron spins and this tends to "short-circuit" the ENDOR mechanism.) We did, however, do a number of control experiments where glycerol was not used; instead we used an excess of diamagnetic CO-liganded heme protein as the magnetic dilutant for the paramagnetic heme protein. As a general rule we obtain better ENDOR percentages with glycerol present, but when glycerol is not present the ENDOR frequencies (i.e., electron densities) are nevertheless unchanged. The one case where glycerol made a substantial difference in the properties of a heme protein was with the carp hemoglobins where glycerol stabilized even up to pH 8 the form of the protein whose EPR spectrum had been associated<sup>6</sup> with low pH. Thus glycerol was *not* used in comparing high- and low-pH forms of carp hemoglobin.

#### High-Spin Ferric Heme. Results, Theory, and Discussion

**Results. Protons of High-Spin Derivatives.** By using the dispersion EPR mode, we brought out new ENDOR reso-

**Table I.** Proton Hyperfine Couplings for High-Spin Aquo- and Fluoromyoglobin Complexes<sup>a,b</sup>

compd	proton assignment	hyperfine coupling, MHz
aquo-Mb	heme-bound H <sub>2</sub> O (Figure 1)	6.02 ± 0.08
aquo-Mb	heme, meso proton (B, B', Figure 2a,b)	0.79 ± 0.008
MbF <sup>-</sup>	heme, meso proton (B, B', Figure 2c,d)	0.82 ± 0.008
aquo-Mb	δ-N proton prox hist (A, A', Figure 2a)	1.33 ± 0.02
MbF <sup>-</sup>	δ-N proton prox hist (A, A', Figure 2c)	1.25 ± 0.03

<sup>a</sup> Spectra were taken near the  $g_z = 2.00$  extremum as discussed in figure legends 1 and 2.  $\nu_{\text{NMR}}$  is in the range 13.80–14.00 MHz depending on the sample. <sup>b</sup> Couplings for the corresponding hemoglobin compounds are in the supplementary material.

nances from exchangeable protons of aquometmyoglobin and aquomethemoglobin which had the large hyperfine splitting of about 6 MHz shown in Figure 1. We assign this ENDOR to heme-bound H<sub>2</sub>O protons as discussed below. Because the proper dispersion ENDOR conditions had not previously been found, such proton ENDOR was not previously reported.<sup>3c</sup> This proton ENDOR is not seen when fluoride is a ligand. (We have noted in Figure 1 broad nonexchangeable proton ENDOR labeled CC' which has the next largest splitting (of about 2 MHz) after the H<sub>2</sub>O protons. We tentatively assign this ENDOR to the CH protons of histidine that are the nearest histidine protons to the heme iron.)

By using dispersion, small field modulation, and slow ENDOR frequency sweeps, we were able to bring in large numbers of weakly coupled protons shown in Figure 2. This was with considerably better signal to noise than obtained in the one instance previously reported for the protons of the heme protein aquometmyoglobin.<sup>3c</sup> Figure 2 compares the ENDOR of protons within ±1.2 MHz of the free proton frequency for aquo- and fluorometmyoglobin. Although there is a good deal of other well-defined detail, the features that we have assigned are the sharp peaks labeled BB' (to meso protons) and the exchangeable proton AA' (to an exchangeable proton on the δ nitrogen of the proximal histidine). As shown in Table I, there is a slight difference in the splitting of the AA' and BB' protons between the fluoro and aquo compounds. The couplings reported in Table I for myoglobin are essentially identical with those for hemoglobin, which are reported in the supplementary material.

**Theory and Discussion. Protons of High-Spin Derivatives.** ENDOR frequencies from a particular type of proton generally appear centered about the bulk free proton frequency,  $\nu_{\text{NMR}}$ . The first-order expression for proton ENDOR frequencies is<sup>3c</sup>

$$\nu_{\text{ENDOR}} = \nu_{\text{NMR}} \pm |A_{zz}|/2 \quad (1)$$

where  $A_{zz}$  is the component of the proton hyperfine coupling parallel here to the heme normal.

The interaction between the electron spin and a proton several ångströms away can often be estimated by a first-order dipolar interaction given by

$$A_{\text{dipole}} = \frac{g_z g_H \beta_c \beta_n}{r^3} (3 \cos^2 \alpha - 1) \quad (2)$$

where  $r$  is the distance between proton and iron and  $\alpha$  is the angle between the direction of the applied magnetic field (along the heme normal here) and the vector from the iron to the

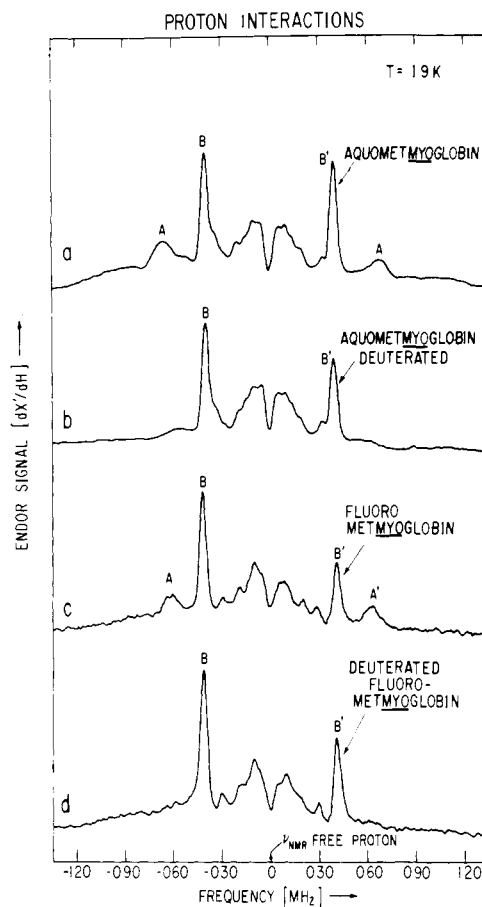


**Figure 2.** A comparison of the weakly coupled proton ENDOR from aquo and fluoro derivatives of metmyoglobin in protonated and deuterated solvents. ENDOR was done at the  $g_z = 2.00$  extremum of the metmyoglobin and on the higher field peak of the  $g_z = 2.00$  fluoride doublet. The experimental conditions are given in the Experimental Section. The solvent system for these spectra was a 1:1 glycerol–buffer, but control experiments were run on the aquo samples without glycerol that showed that the exchangeable proton AA' was still present. The aquo derivatives took about 25 min of signal averaging and the fluoro derivatives about 2 h. We have referred each spectrum to its respective free proton frequency.

proton.  $g_z$  is the electronic  $g$  factor along the heme normal.  $g_H$  is the proton nuclear  $g$  factor, and  $\beta_c$  and  $\beta_n$  are respectively the electronic and nuclear Bohr magnetons. The coordinates of the carbons, nitrogens, oxygens, and iron are obtained from X-ray crystallography of myoglobin.<sup>10,11</sup> To calculate the position of the heme-bound water molecule, we took an Fe–O bond length of 2.15 Å from Watson<sup>10</sup> and HOH bond length and bond angle of 0.96 Å and 104.5°, respectively, from Pauling.<sup>12</sup> The water molecule was symmetrically arranged along the heme normal as shown in Figure 3, which also shows the resultant distance to water protons, the angle  $\alpha$  for water protons, and the calculated dipolar interaction for water protons. Even if the water bond angles and iron–proton distance should be slightly distorted away from the rather symmetric structure of Figure 3, the dipolar coupling to the water protons is larger by far than the coupling to any other possible exchangeable proton. Therefore, the ENDOR signals labeled heme-bound water in Figure 1 must be from heme-bound water. We were surprised at how well the simple point dipole interaction between proton and electron spin on the iron accounts for the observed ENDOR splittings of the heme-bound water protons, independent of any covalent contribution.

In Figure 2 the nonexchangeable peaks BB' are highly reminiscent in both splitting and shape to meso proton peaks seen in our model hemin studies.<sup>3c</sup> Porphyrins lacking meso protons do not give such peaks. The splitting of these peaks is

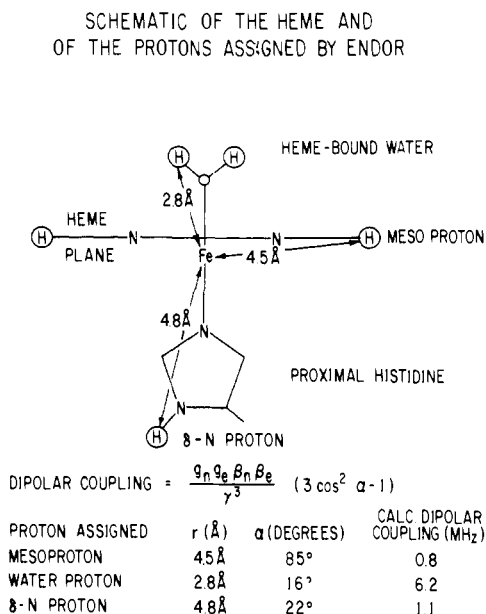


**Figure 3.** A schematic drawing indicating the protons assigned from ENDOR work on high-spin ferric heme protons. Heme coordinates are from ref. 10.

well predicted by dipolar coupling (eq 2). As indicated in Table I, there is a slightly larger splitting of the meso proton ENDOR from the fluoroprotein than from the aquo. Our previous model studies have shown that these meso proton couplings are somewhat sensitive to the nature of the axial ligand.<sup>3c</sup>

We had already seen a considerably larger coupling to the water proton than the coupling exhibited by the exchangeable protons AA', and the splitting of the peaks AA' was only slightly affected by the change in axial ligand from fluoro to aquo. Thus it was necessary to look beyond the heme iron's sixth ligand environs for an exchangeable proton which would still be close enough to the iron to cause the coupling of 1.2–1.3 MHz seen for AA' protons. The proton attached to the δ nitrogen of the proximal histidine is the next nearest exchangeable proton after the water proton and seems the best candidate for AA'.<sup>13</sup> The dipolar interaction with this proton substantially accounts for the observed splittings of AA'. The excess of the observed hyperfine coupling over the calculated dipolar coupling could arise from a small covalent contribution.

For the two nearest histidine CH protons, which we tentatively assign to CC' of Figure 1, we calculate a dipolar interaction in the 1–2-MHz range from eq 2. The center of gravity of the CC' ENDOR signal appears slightly above  $\nu_{\text{NMR}}$ . Because the histidine CH's lie quite far off the heme normal ( $\alpha \sim 30\text{--}45^\circ$ ), they would have a fairly large second-order dipolar term in  $\sin(2\alpha)$  which would shift the center of gravity above  $\nu_{\text{NMR}}$ .

**Results. Nitrogens of Fluoride Derivatives.** Nitrogen ENDOR has previously been seen in many high-spin ferric heme systems and histidine nitrogen ENDOR seen from aquometmyoglobins and methemoglobins.<sup>3a,c</sup> The general features of the nitrogen ENDOR from fluorometmyoglobin and methemoglobin are similar to those from the corresponding aquo compounds. The main difference is that the readily identifiable higher frequency histidine peaks occur near 6.0 and 8.0 MHz, each being about 0.5 MHz lower in frequency than their counterparts on the aquo-liganded proteins.<sup>14</sup> This is an apparent manifestation of a trans effect of the fluoro ligand upon the proximal histidine.

### Low-Spin Ferric Heme. Results, Theory and Discussion

**Results.  $^{13}\text{CN}^-$  Metmyoglobin and Methemoglobin.** Figure

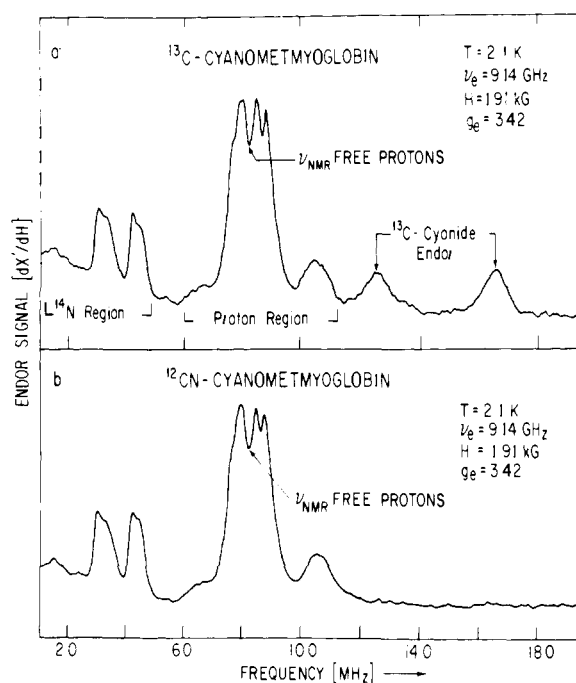


**Figure 4.** A comparison of ENDOR from cyanometmyoglobin prepared with  $^{13}\text{CN}^-$  and  $^{12}\text{CN}^-$ . Spectra were taken with about 30 min of signal averaging. Spectra were taken near the  $g_z$  extremum where the magnetic field is essentially along the heme normal.

4 compares the ENDOR signals from metmyoglobin cyanides made respectively with  $^{13}\text{CN}^-$  ( $I = 1/2$ ) or with  $^{12}\text{CN}^-$  ( $I = 0$ ). Two new ENDOR resonances appear from the  $^{13}\text{CN}^-$  material, and, as indicated in Table II, these lines have the appropriate Zeeman splitting for  $^{13}\text{C}$  at the fields used. We have compared the  $^{13}\text{CN}^-$  ENDOR of metmyoglobin with that from methemoglobin, and we find the  $^{13}\text{C}$  coupling for hemoglobin to be about 1.5 MHz lower than that of metmyoglobin. Perhaps this small difference reflects the difference in the axial ligand binding site between hemoglobin and myoglobin.<sup>15</sup>

The best estimates for  $A$  on a frozen solution are the values of  $A_z$  measured at the  $g_z$  extremum. However, we have followed the behavior of the  $^{13}\text{CN}^-$  ENDOR lines on going to  $g$  values below the  $g_z = 3.4$  extremum down as far as an electronic  $g$  value of about 2.0. Although there is considerable broadening of the ENDOR lines, as would be expected in a frozen solution away from the  $g_z$  extremum, the frequency of the ENDOR lines stayed fairly constant. We suspect that the major portion of the  $^{13}\text{CN}^-$  hyperfine coupling is isotropic, although exact details will have to await future single-crystal work.

**Theory and Discussion.  $^{13}\text{CN}^-$ .** The first-order spin Hamiltonian for  $^{13}\text{CN}^-$ , which here has a larger electron–nuclear hyperfine interaction than nuclear Zeeman interaction, is given by

$$\nu_{\text{ENDOR}} = |A/2| \pm g_c \beta_n H \quad (3)$$

Thus one expects a pair of  $^{13}\text{C}$  lines split by the appropriate values of  $2g_c \beta_n H$  given in Table II.

Although no  $^{13}\text{CN}^-$  hyperfine couplings have yet been reported from  $^{13}\text{C}$  NMR on heme proteins, a chemical shift of +2400 ppm (meaning a negative contact interaction) has been reported from dicyanohemins.<sup>16</sup> If the  $^{13}\text{CN}^-$  hyperfine coupling that we have measured here is strictly isotropic, then we would predict a  $^{13}\text{CN}^-$  chemical shift at 300 K of about 3000 ppm in magnitude for metmyoglobin cyanide. A comparable contact interaction measured by NMR<sup>17,18</sup> was reported for  $[\text{Fe}(^{13}\text{CN})_6]^{3-}$ , and similar isotropic couplings have been re-

Table II.  $^{13}\text{CN}^-$  Hyperfine Couplings<sup>a</sup>

compd	ENDOR frequencies, MHz	hyperfine couplings, $ A_{zz} $ MHz
Mb $^{13}\text{CN}$ at $g_z = 3.42$ $H = 1.91$ kG $2g_C\beta_n H = 4.08$ MHz	$12.30 \pm 0.05$ $16.34 \pm 0.05$	$28.64 \pm 0.08$
Hb $^{13}\text{CN}$ at $g_z = 3.50$ $H = 1.86$ kG $2g_C\beta_n H = 3.98$ MHz	$11.70 \pm 0.16$ $15.63 \pm 0.08$	$27.33 \pm 0.18$

<sup>a</sup> These samples were prepared in 1:1 (v/v) glycerol-buffer solution as described in the Experimental Section.

ported for  $^{13}\text{CN}^-$  complexes of other transition metals.<sup>19</sup> Single-crystal EPR on  $[\text{Cr}(^{13}\text{CN})_6]^{3-}$  has shown that the anisotropic contribution to the  $^{13}\text{CN}$  hyperfine interaction is smaller than the isotropic interaction.<sup>19</sup> It has been suggested that a large  $^{13}\text{CN}^-$  contact interaction of negative sign could arise from an exchange polarization mechanism between unpaired metal d electrons and paired electrons in a cyanide  $\sigma$  orbital.<sup>19</sup> In any case, the magnitude of the hyperfine results for  $^{13}\text{CN}^-$  attached to the heme iron is in substantial agreement with hyperfine couplings for other transition metal cyanide complexes, couplings which happen to be largely isotropic and of negative sign.

**Results. Proton ENDOR of the Cyanide Complexes.** Figure 5 compares the proton ENDOR spectra from protohemin cyanide with those of metmyoglobin and hemoglobin cyanides. This figure points out that the outlying ENDOR lines with hyperfine coupling of about 1.75 MHz and labeled "Ex" for both myoglobin and hemoglobin are exchangeable. The lines labeled 3 for the protohemin and C for the myoglobin and hemoglobin are most likely from the meso protons of the heme.<sup>3f</sup> There is a decrease in the hyperfine coupling of these meso proton lines from 1.43 to 1.34 to 1.19 MHz on going from protohemin to hemoglobin to myoglobin. We also note that the ENDOR lines, notably those of the meso protons, are considerably sharper in hemoglobin than in myoglobin. A detailed table of proton hyperfine couplings for the cyanide complexes is given in the supplementary material (Table I-S).

If we base our judgment on a comparison with the protohemin cyanide spectrum, it appears that several other ENDOR lines in myoglobin and hemoglobin nearer the free proton frequency could arise from heme protons. We have also noted in myoglobin and hemoglobin broad, outlying, nonexchangeable proton resonances split by about 4 MHz, which are best observed in the wider sweeps of Figure 4; these move along with the protons as we change magnetic field. We suspect that these are the near-CH protons of the proximal histidine.

We have observed proton ENDOR from protons in hemoglobin and myoglobin azide, and this ENDOR is not so sharply resolved as the proton ENDOR from the cyanide compounds. The meso proton splitting in the azide compounds from both hemoglobins and myoglobins appears to be about 1.00 MHz.

**Theory and Discussion. Proton ENDOR of the Cyanide Complexes.** We have previously published proton spectra of protohemin cyanide in DMF and of metmyoglobin which was in protonated aqueous solvent.<sup>3f</sup> Based on known small meso proton NMR contact shifts<sup>20</sup> and upon our own calculation of the dipolar coupling (eq 2 with  $g_z \approx 3.5$ ) between meso proton and the spin on the iron (about  $-1.5$  MHz dipolar coupling), we had previously assigned lines marked 3 in Figure 5a and C in Figure 5e to the meso protons.<sup>3f,21</sup> We likewise

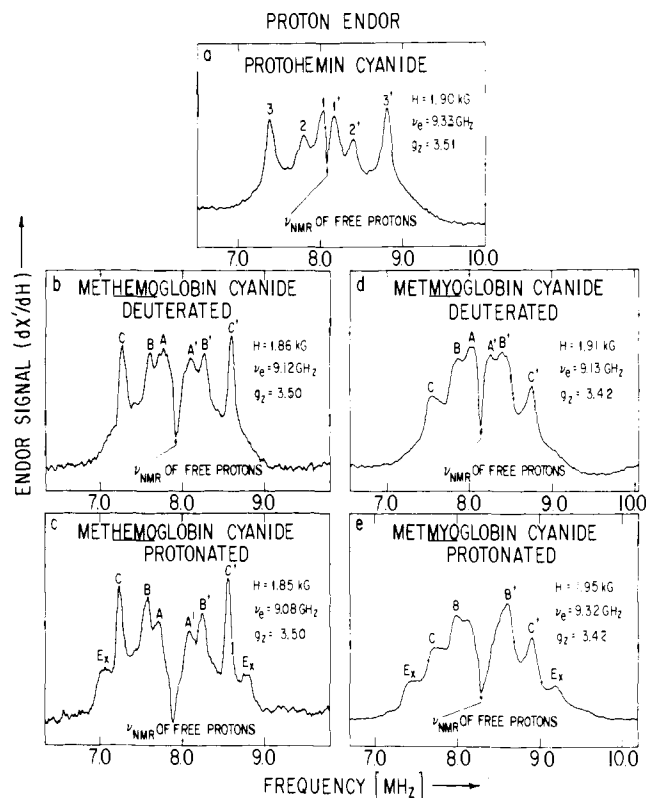


**Figure 5.** Comparison of weakly coupled proton ENDOR from the cyanide derivatives of protohemin, metmyoglobin, and methemoglobin. The magnetic field is at the  $g_z$  extremum. ENDOR conditions are similar to those described for weakly coupled protons in the Experimental Section. The protohemin cyanide was 6 mM in protohemin dissolved in freshly distilled DMF and was about 0.1 M in KCN that had initially been dissolved in a drop of  $\text{D}_2\text{O}$ . The proteins were about 5 mM in heme and were dissolved in glycerol-buffer. Spectra (a) and (e) are similar to those shown in ref 3f. The spectra took 0.5–1.0 h of signal averaging.

assign here the lines marked in C in Figure 5b,c,d to meso protons. The experimental difference in meso proton couplings between the three cyanide compounds is larger than would be predicted just from the effect of their slightly different electronic  $g$  values on the dipolar interaction. Thus, the difference between the meso proton couplings in these three compounds may reflect a difference in covalent couplings. Regarding the relative sharpness of the hemoglobin meso proton ENDOR vs. that of the myoglobin, we suspect that this sharpness reflects more nearly electronically equivalent meso protons in hemoglobin.

The most likely candidates for the exchangeable protons "Ex" with splitting of 1.75 MHz in the proteins would be either the proton on the  $\delta$  nitrogen of the proximal histidine or else a proton that is hydrogen bonded to the cyanide.<sup>22</sup> The calculated dipolar coupling to the  $\delta$  proton 4.8 Å away (see Figure 3) would be about 1.9 MHz. In previous unpublished studies on protohemin cyanide in DMF we found that if we used KCN dissolved in a small amount of  $\text{H}_2\text{O}$  (rather than  $\text{D}_2\text{O}$  as in Figure 5a) to make our protohemin cyanide, a pair of new exchangeable protons with hyperfine splitting of about 2.6 MHz appeared. In the protohemin cyanide model it is therefore highly likely that an exchangeable proton could bind to the cyanide. The dipolar coupling to such a proton 4.5 Å exactly along the heme normal is calculated to be about 3.0 MHz and to a proton 5.5 Å along the heme normal is calculated at 1.6 MHz. Thus, whether the observed, exchangeable proton is on the proximal histidine or hydrogen bonded to the cyanide, its distance is in the 4.5–5.5-Å range.

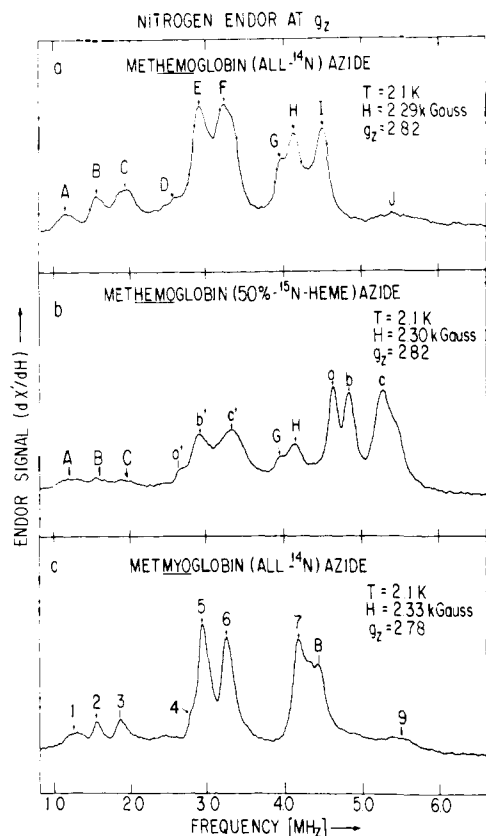


**Figure 6.** A comparison of the nitrogen ENDOR at  $g_z$  from the azide derivatives of all- $^{14}\text{N}$  methemoglobin (a), methemoglobin containing 50%  $^{15}\text{N}$  on the heme (b), and all- $^{14}\text{N}$  metmyoglobin (c). The proteins in (a) and (c) were about 5 mM in heme while the  $^{15}\text{N}$  hemoglobin was about 1 mM. ENDOR conditions were similar to those of Figure 1. Figure 6a took 30 min signal averaging; (b), 2 h; (c), 15 min. Peaks are labeled for identification with the data of Table III. In (b) the peaks a,a'; b,b'; c,c' are split by the appropriate value of the  $^{15}\text{N}$  Zeeman splitting,  $2^{15}g_N\beta_N H = 1.99$  MHz. A, B, C, G, H in (b) are from residual  $^{14}\text{N}$ . Controls were run for spectra (a) and (c) with a solution free of glycerol but with excess diamagnetic heme protein as a magnetic dilutant; these control spectra were very similar to those shown, although individual peaks were slightly broader.

**Results. Nitrogen ENDOR from Heme Protein Azides. A. Methemoglobin and Sperm Whale Metmyoglobin Azides.** When we looked at the nitrogen ENDOR from these compounds, we found (apparently because of favorable relaxation rates) ENDOR with excellent signal to noise and resolution. ENDOR with good resolution was obtained not only at the  $g_z$  extremum as in Figure 6 but also at the high-field  $g_x$  extremum as in Figure 7. Even though the  $g$  values of methemoglobin and metmyoglobin azides are quite similar ( $g_z, g_y, g_x = 2.82, 2.21, 1.69$  for hemoglobin and  $2.78, 2.21, 1.74$  for myoglobin) we noted at  $g_x$  substantial differences in their ENDOR spectra. Although the general features of nitrogen ENDOR from cyanide and azide compounds are similar at  $g_z$ , we found better resolved detail from the azide compounds, especially of the weaker peaks in the 1–2-MHz region.

By using the hemoglobin enriched to 50% in  $^{15}\text{N}$  heme, we have attempted to assign the many observed ENDOR lines. Because of the effect of the quadrupole interaction with the  $I = 1$  nucleus of  $^{14}\text{N}$ ,  $^{15}\text{N}$  ( $I = 1/2$ ) will generally give simpler ENDOR spectra with fewer overlapping transitions. On going to the hemoglobin with 50% enrichment in  $^{15}\text{N}$  only on the heme, we saw the appearance of  $^{15}\text{N}$  Zeeman pairs<sup>23</sup> and a decrease in the intensity of the other ENDOR resonances which had previously been seen in studies of all- $^{14}\text{N}$  hemoglobin and myoglobin. Thus, heme nitrogens contribute to the nitrogen ENDOR from the heme protein azides.

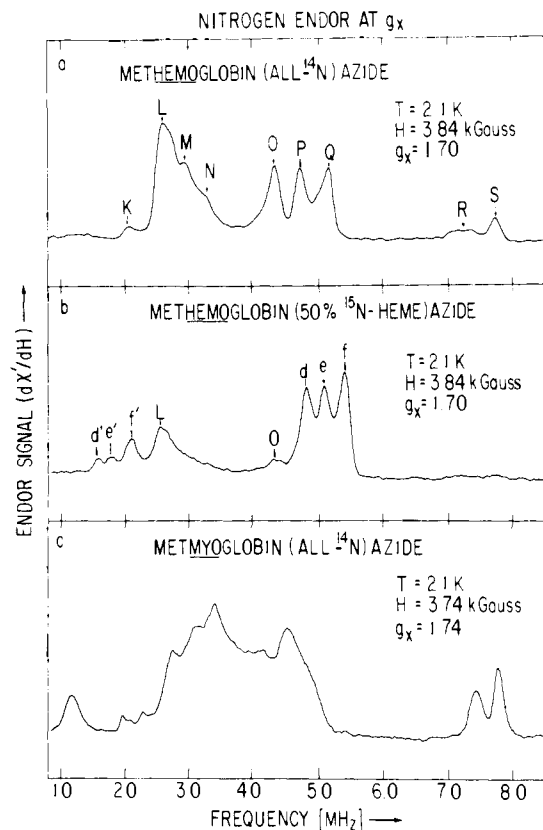


**Figure 7.** ENDOR spectra at  $g_x$  in the heme plane from the same samples as in Figure 6. In (b) the peaks d,d'; e,e'; f,f' are split by the appropriate value of the  $^{15}\text{N}$  Zeeman splitting,  $2^{15}g_N\beta_N H = 3.31$  MHz. L and O in (b) are from residual  $^{14}\text{N}$ . (a) and (b) took about 30 min signal averaging while (c) took 15 min.

Given the complex nitrogen spectra, we were concerned that there might be at least some ENDOR from  $^{14}\text{N}$  not on the heme; for example, on the histidine or on the azide. To discover an azide nitrogen contribution, we looked at hemoglobin and myoglobin made with  $^{15}\text{N}$  azide, but not with  $^{15}\text{N}$  heme. We found at best a weak new peak near 2.25 MHz at  $g_z$  in myoglobin and no apparent changes in the intensity of previously observed  $^{14}\text{N}$  ENDOR. This still left histidine as a potential contributor to some of the ENDOR found both in all- $^{14}\text{N}$  hemoglobin and in 50% heme hemoglobin. Thus, we examined in detail the behavior of the spectral features in the two isotopically different hemoglobins. Peaks such as B, C, E, F, G, H (Figure 6a) and L, M, N, O, R, S (Figure 7a) were lower in intensity in the  $^{15}\text{N}$ -heme hemoglobin; so they must be from  $^{14}\text{N}$  heme. (We estimated intensity changes of peaks by comparing them to the "internal standard" of the proton ENDOR.) In the 3-MHz region of Figures 6a and 6b there is overlap of  $^{14}\text{N}$  and  $^{15}\text{N}$  peak positions, but here the intensity of resultant peaks in the  $^{15}\text{N}$  hemoglobin appears to be down from where it would be if the peaks were from a commonly shared, non-heme  $^{14}\text{N}$  nitrogen. In the 4–5-MHz region there were ENDOR peaks at  $g_x$  and  $g_z$  occurring both in the all- $^{14}\text{N}$  material and in the 50%  $^{15}\text{N}$  heme material; although the frequencies of such peaks were not identical for the two isotopically different hemoglobins, they were fairly close. In the all- $^{14}\text{N}$  material we found that peaks (G, H, I of Figure 6a and O, P, Q of Figure 7a) which started in the 4–5 MHz region at the  $g$ -value extremes moved to lower ENDOR frequencies at intermediate  $g$  values and lost resolution. In the  $^{15}\text{N}$  hemoglobin the peaks (a, b, c of Figure 6a and d, e, f of Figure 7b) which started in the 4–5-MHz region at the  $g$ -value extremes stayed near 5 MHz and remained fairly well resolved at intermediate  $g$  values. Thus, those peaks which occur in the

4–5-MHz region from both  $^{14}\text{N}$  and  $^{15}\text{N}$  protein do not behave as if they came from a commonly shared, nonheme  $^{14}\text{N}$ ; they are from heme nitrogen. Indeed, with possible exceptions of weak peaks A and J of Figure 6a, we conclude that the observed spectral features that we have seen belong to the heme nitrogens. Given the complex dependence of ENDOR signals on many experimental conditions (relaxation, power, modulation),<sup>3c</sup> we certainly cannot rule out the possibility of ever finding ENDOR from histidine nitrogen under different conditions, and we intend in the future to look with higher rf powers and at higher temperatures for histidine nitrogen.

**B. Carp Hemoglobin Azides.** The carp hemoglobin azides underwent a change in  $g$  values from  $g_z, g_y, g_x = 2.84, 2.20, 1.68$  in the high-pH form to  $2.91, 2.20, 1.64$  in the low-pH form. We had noted a comparable  $g$ -value change in going from myoglobin to hemoglobin, and we had seen the substantial changes in nitrogen ENDOR between hemoglobin and myoglobin, especially at  $g_x$ . At the  $g_x$  and  $g_z$  extremes we looked in detail at the ENDOR of the carp hemoglobins. Even though the  $g$  values occurred as previously reported,<sup>6</sup> we were unable to detect any substantial difference in the ENDOR spectra. Figure 8 shows the ENDOR spectra of the two forms measured at  $g_x$  in a frequency region where (based on hemoglobin vs. myoglobin) we had particularly expected to find ENDOR differences. For both high- and low-pH forms there are two well-defined peaks (o, q) in the 4–5-MHz region, and there is a slight hint of a shoulder between the two peaks. There is at best a slight difference in the shape of this intermediate shoulder between the two forms of carp hemoglobin. (In the human hemoglobin which has about the same  $g$  values as the high-pH carp hemoglobin we had noted *three* well-defined peaks (O, P, Q of Figure 7a) in the 4–5-MHz region.) We believe on the basis of our  $^{14}\text{N}$ – $^{15}\text{N}$  assignment work that these peaks are all from heme nitrogens of carp hemoglobin.

**Theory and Discussion. Nitrogen ENDOR from Heme Protein Azides. A. Methemoglobin and Metmyoglobin Azides.** Although we can assign most of the spectral features of these azide complexes to heme nitrogens, the nitrogen ENDOR from them is difficult to analyze in detail, particularly for the all- $^{14}\text{N}$  material. There are a large number of lines, some partially overlapping; there certainly are more lines than just the single set of four lines that would be expected for one set of equivalent  $^{14}\text{N}$ 's or the two lines for one set of  $^{15}\text{N}$ 's.<sup>3a</sup> The underlying reason for the large number of lines is the likely electronic inequivalence of heme nitrogens even on the same heme molecule, and we discuss this possibility in the supplementary appendix. (When we had previously done ENDOR with the magnetic field along the heme normal in high-spin ferric hemes,<sup>3a-c</sup> we had not found obvious effects of heme nitrogen inequivalence, apparently because of the fourfold electronic symmetry at the heme iron in high-spin ferric hemes.) There is, of course, the additional possibility for  $\alpha$ – $\beta$  inequivalence in hemoglobins.

When we are doing ENDOR at the  $g_x$  extremum we are looking in the heme plane in a direction which, as shown by myoglobin azide single-crystal EPR,<sup>24</sup> does not coincide with iron nitrogen bond directions. Thus, the  $g_x$  direction does not coincide with expected principal axis directions for the nitrogen hyperfine or quadrupole tensors. Complications from such noncollinearity of axes are discussed in the supplementary appendix.

We have previously used a simple first-order spin Hamiltonian to interpret our nitrogen ENDOR in high-spin ferric hemes. Such a Hamiltonian had a minimal number of parameters which were easily fit to ENDOR data at the  $g_z = 2.00$  extremum in high-spin ferric hemes.<sup>3a-c</sup> The first-order spin Hamiltonian has the form given by eq 4 and 5 for  $^{14}\text{N}$  and  $^{15}\text{N}$ , respectively. In the supplementary appendix the first-order Hamiltonian is related to a more general spin Hamilto-

CARP HEMOGLOBIN: HIGH pH FORM vs LOW pH FORM

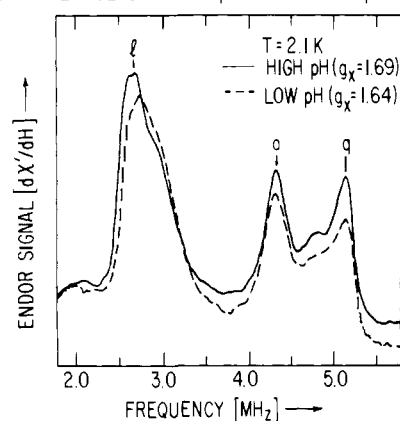


**Figure 8.** A comparison of the nitrogen ENDOR from carp hemoglobin azides in the high- and low-pH form. Spectra were taken at the  $g_x$  extrema. The solvent system was buffer *free* from glycerol. The buffer for the low-pH form was 0.05 M citrate-phosphate, pH 4.8, and for the high-pH form was 0.05 M sodium phosphate, pH 8.0. Each spectrum took about 40 min of signal averaging. The peaks labeled l, o, and q occur near 2.6, 4.3, and 5.1 MHz, respectively.

nian for nitrogen:

$$\mathcal{H}^{14} = {}^{14}A_{zz}I_zS_z + P_{zz}[I_z^2 - \frac{1}{3}I(I+1)] - {}^{14}g_N\beta_nH_zI_z \quad (4)$$

$$\mathcal{H}^{15} = {}^{15}A_{zz}I_zS_z - {}^{15}g_N\beta_nH_zI_z \quad (5)$$

The  $z$  axis here is the direction of the  $g_z$  axis, approximately normal to the heme plane. For hyperfine effects along the  $g_x$  axis we can formally write a first-order spin Hamiltonian similar to that of eq 4 or 5 except for a change in the subscript label. The resultant first-order expressions for  $\Delta I = I$  ENDOR transition frequencies are

$$[\frac{1}{2}|{}^{14}A_{zz}| + |P_{zz}| + {}^{14}g_N\beta_nH] \quad (6a-1)$$

$$({}^{14}\text{N}) \nu_{\text{ENDOR}} = [\frac{1}{2}|{}^{14}A_{zz}| - |P_{zz}| + {}^{14}g_N\beta_nH] \quad (6a-2)$$

$$[\frac{1}{2}|{}^{14}A_{zz}| + |P_{zz}| - {}^{14}g_N\beta_nH] \quad (6a-3)$$

$$[\frac{1}{2}|{}^{14}A_{zz}| - |P_{zz}| - {}^{14}g_N\beta_nH] \quad (6a-4)$$

$$({}^{15}\text{N}) \nu_{\text{ENDOR}} = [\frac{1}{2}|{}^{15}A_{zz}| \pm {}^{15}g_N\beta_nH] \quad (6b)$$

When first-order expressions hold, we expect to see pairs of ENDOR lines separated by the appropriate values of  $2g_N\beta_nH$ . (Values for  $2g_N\beta_nH$  are included in Table III.) Indeed such a separation of lines is quite accurately seen for  $^{15}\text{N}$  lines in hemoglobin azides, where both lines of the  $^{15}\text{N}$  Zeeman pair appear with adequate resolution and signal to noise, even though the lower frequency member of a pair is invariably the weaker in intensity. In both  $^{14}\text{N}$  hemoglobin and myoglobin, a number of obvious  $^{14}\text{N}$  Zeeman pairs also occur; e.g., the pairs 2,5; 3,6 (Figure 6c) in myoglobin and B,E; C,F (Figure 6a) in hemoglobin.

Our pragmatic approach to extracting the spin Hamiltonian parameters was to fit the simpler  $^{15}\text{N}$  data first. The hyperfine couplings  $|{}^{15}A_{zz}|$  for the three pairs of  $^{15}\text{N}$  Zeeman lines, a,a'; b,b'; c,c', of Figure 6b are respectively 7.26, 7.72, 8.58 ( $\pm 0.05$ ) MHz. Since we knew the nuclear  $g$  values<sup>25</sup> of both  $^{14}\text{N}$  and  $^{15}\text{N}$ , we then could back-calculate expected  $^{14}\text{N}$  hyperfine couplings. The back-calculated  $^{14}\text{N}$  values turned out to be 5.17, 5.50, and 6.12 MHz. We then attempted to find sets of  $^{14}\text{N}$  lines which would give reasonable agreement with these back-calculated  $^{14}\text{N}$  hyperfine values. Because of considerable overlap of  $^{14}\text{N}$  ENDOR lines, it was not always easy to find a complete set of four distinct resonances to fit the four ex-

Table III. Nitrogen ENDOR of Methemoglobin and Metmyoglobin Azides

compd and conditions	ENDOR frequencies, MHz, and assignments	derived couplings, MHz
HbN <sub>3</sub> <sup>-</sup> -50% <sup>15</sup> N on heme <i>g</i> <sub>z</sub> = 2.82 <i>H</i> = 2.30 kG <sup>215</sup> <i>g</i> <sub>Nβ<sub>n</sub></sub> <i>H</i> = 1.99 MHz	(see Figure 6b)	
	2.65 ± 0.04 (a') 4.61 ± 0.02 (a) } heme <sup>15</sup> N	<sup>15</sup> <i>A</i> <sub>zz</sub>   = 7.26 ± 0.05
	2.90 ± 0.04 (b') 4.82 ± 0.02 (b) } heme <sup>15</sup> N	<sup>15</sup> <i>A</i> <sub>zz</sub>   = 7.72 ± 0.05
	3.31 ± 0.04 (c') 5.27 ± 0.02 (c) } heme <sup>15</sup> N	<sup>15</sup> <i>A</i> <sub>zz</sub>   = 8.58 ± 0.05
HbN <sub>3</sub> <sup>-</sup> -all <sup>14</sup> N <i>g</i> <sub>z</sub> = 2.82 <i>H</i> = 2.29 kG <sup>214</sup> <i>g</i> <sub>Nβ<sub>n</sub></sub> <i>H</i> = 1.41 MHz	(see Figure 6a)	(B, E, G) yield   <sup>14</sup> <i>A</i> <sub>zz</sub>   = 5.39   <i>P</i> <sub>zz</sub>   = 0.51
	1.14 ± 0.05 (A)	
	1.51 ± 0.02 (B) heme	
	1.86 ± 0.04 <sup>a</sup> (C) heme	(C, F, H) yield   <sup>14</sup> <i>A</i> <sub>zz</sub>   = 5.87   <i>P</i> <sub>zz</sub>   = 0.41
	2.6 ± 0.1 (D) heme	
	2.86 ± 0.02 (E) heme	
	3.18 ± 0.02 <sup>a</sup> (F) heme	
	3.91 ± 0.02 (G) heme	
	4.05 ± 0.02 (H) heme	(C, F, I) yield   <sup>14</sup> <i>A</i> <sub>zz</sub>   = 6.25   <i>P</i> <sub>zz</sub>   = 0.06
4.43 ± 0.02 (I) heme		
5.35 ± 0.02 (J)		
MbN <sub>3</sub> <sup>-</sup> -all <sup>14</sup> N <i>g</i> <sub>z</sub> = 2.78 <i>H</i> = 2.33 kG <sup>214</sup> <i>g</i> <sub>Nβ<sub>n</sub></sub> <i>H</i> = 1.44 MHz	(see Figure 6c)	(2, 5, 7) yield   <sup>14</sup> <i>A</i> <sub>zz</sub>   = 5.64   <i>P</i> <sub>zz</sub>   = 0.62
	1.13 ± 0.06 (a)	
	1.48 ± 0.03 (2) heme	
	1.81 ± 0.03 (3) heme	
	2.74 ± 0.04 (4) heme	(3, 6, 8) yield   <sup>14</sup> <i>A</i> <sub>zz</sub>   = 6.14   <i>P</i> <sub>zz</sub>   = 0.55
	2.91 ± 0.02 (5) heme	
	3.23 ± 0.02 (6) heme	
	4.16 ± 0.02 (7) heme	
	4.34 ± 0.02 (8) heme	
5.45 ± 0.02 (9)		
HbN <sub>3</sub> <sup>-</sup> -50% <sup>15</sup> N on heme <i>g</i> <sub>x</sub> = 1.70 <i>H</i> = 3.84 kG <sup>215</sup> <i>g</i> <sub>Nβ<sub>n</sub></sub> <i>H</i> = 3.31 MHz	(see Figure 7b)	
	1.50 ± 0.04 (d') 4.79 ± 0.02 (d) } heme <sup>15</sup> N	<sup>15</sup> <i>A'</i> <sub>xx</sub>   = 6.29 ± 0.05
	1.73 ± 0.04 (e') 5.03 ± 0.02 (e) } heme <sup>15</sup> N	<sup>15</sup> <i>A'</i> <sub>xx</sub>   = 6.76 ± 0.05
	2.03 ± 0.04 (f') 5.39 ± 0.02 (f) } heme <sup>15</sup> N	<sup>15</sup> <i>A'</i> <sub>xx</sub>   = 7.42 ± 0.05
HbN <sub>3</sub> <sup>-</sup> -all <sup>14</sup> N <i>g</i> <sub>x</sub> = 1.70 <i>H</i> = 3.84 kG <sup>214</sup> <i>g</i> <sub>Nβ<sub>n</sub></sub> <i>H</i> = 2.35 MHz		details of coupling in supplementary appendix
	1.99 ± 0.04 (K) heme	
	2.52 ± 0.02 (L) heme	
	2.86 ± 0.04 (M) heme	
	3.18 ± 0.04 (N) heme	
	4.27 ± 0.02 (O) heme	
	4.67 ± 0.02 (P) heme	
	5.09 ± 0.02 (Q) heme	
7.14 ± 0.1 (R) heme 7.65 ± 0.04 (S) heme		

<sup>a</sup> Closer observation with signal averaging over a narrow range indicates two peaks split by about 0.10 MHz. <sup>b</sup> These are the *effective* hyperfine couplings along the *g*<sub>x</sub> axis as discussed in the appendix. The prime indicates that these couplings are measured along the *g*<sub>x</sub> axis (i.e., the *X'* axis of Figure S1 of the appendix).

pressions of eq 6a. The following sets of <sup>14</sup>N ENDOR lines gave reasonable agreement with <sup>14</sup>N hyperfine couplings back-calculated from <sup>15</sup>N couplings: (B,E,G), (C,F,H), and (C,F,I) in Figure 6a. We fit these respective sets of three lines to eq 6a-1,2,4. The respective pairs of hyperfine |<sup>14</sup>*A*<sub>zz</sub>| and quadrupole couplings |*P*<sub>zz</sub>| for these sets of lines were (5.39, 0.51), (5.87, 0.41), and (6.25, 0.60) MHz. (The fourth ENDOR line for each set was predicted by eq 6a-3 to be in the 2.6–3.0-MHz region; near 2.6 MHz there is a shoulder D and near 3 MHz there is the intense transition E.) In the myoglobin the sets of lines (2,5,7), (3,6,8) of Figure 6c respectively gave |<sup>14</sup>*A*<sub>zz</sub>| and |*P*<sub>zz</sub>| of (5.64, 0.72) and (6.14, 0.55) MHz.

Based on this analysis we believe that it is accurate to say that for the heme nitrogens the magnetic hyperfine parameter |<sup>15</sup>*A*<sub>zz</sub>| is in the 7.0–8.5-MHz range, while for <sup>14</sup>N the magnetic hyperfine coupling is in the 5.0–6.5-MHz and the quadrupole coupling |*P*<sub>zz</sub>| in the 0.4–0.6-MHz range. Agreement between <sup>14</sup>N and <sup>15</sup>N parameters is not perfect. This may be because the measured <sup>14</sup>N hyperfine parameter actually includes a second-order increment from quadrupole effects. Of course one could conceivably have chosen different sets of <sup>14</sup>N ENDOR lines in the fitting process, though we think our present choice is the best.

At *g*<sub>x</sub> we found the <sup>14</sup>N spectrum more difficult to analyze

because of its complexity (especially in myoglobin) and because of lack of obvious Zeeman-split  $^{14}\text{N}$  lines. In previous work in connection with single-crystal ENDOR of high-spin ferric aquometmyoglobin,<sup>3c</sup> the best resolved, most interpretable ENDOR spectra *in the heme plane* were found with the magnetic field along iron–heme nitrogen bond directions; apparently such bond directions are principal axis direction for quadrupole and hyperfine tensors. When the magnetic field in this previous work made an angle in the 25–45° range with iron–nitrogen bonds, complex spectra occurred which would have been difficult to interpret in the absence of ENDOR at other orientations; this likewise seems the case here. In the present work second-order perturbations may also present further complications, as discussed in the supplementary appendix.

In contrast to the  $^{14}\text{N}$  ENDOR, the  $^{15}\text{N}$  ENDOR at  $g_x$  gave readily observable Zeeman pairs  $d,d'$ ;  $e,e'$ ;  $f,f'$  in Figure 7b, and these gave respective hyperfine couplings of 6.29, 6.76, and 7.42 ( $\pm 0.05$ ) MHz. The closeness of these hyperfine couplings to those measured in the  $g_z$  direction and our ability to follow resolved  $^{15}\text{N}$  lines at  $g$  values intermediate between  $g_x$  and  $g_z$  imply that the heme nitrogen magnetic hyperfine coupling is quite isotropic (at least  $\sim 80\%$ ) in nature. A Fermi interaction from an exchange polarization mechanism may well account for a substantial fraction of the nitrogen hyperfine coupling, just as such a mechanism seems to account for a large fraction of  $^{13}\text{CN}^-$  hyperfine coupling. Having obtained  $^{15}\text{N}$  hyperfine parameters for hemoglobin at  $g_x$ , we attempted to use these to estimate  $^{14}\text{N}$  parameters for hemoglobin. We discuss the details of this attempt in the supplementary appendix. At this time we do not attempt to fit  $^{14}\text{N}$  parameters for myoglobin at  $g_x$ .

A major finding of the azide ENDOR study (independent of the exact details of data analysis) is that the heme nitrogens are electronically inequivalent. There are at least two inequivalent heme nitrogens from myoglobin and at least three in the hemoglobin. Some of the inequivalence in the hemoglobin may be  $\alpha$ – $\beta$  inequivalence. Thus it will be interesting to observe the ENDOR from individual  $\alpha$  and  $\beta$  chains of hemoglobin. Our approach with the azides has been to obtain the well-defined spectra of Figures 6 and 7 and to assign these spectra. That brings us to a point where at least we will be able to use such spectra as probes for biological changes. Insofar as possible we have obtained estimates of hyperfine and quadrupole parameters, taking advantage of correlations which should exist between  $^{15}\text{N}$  and  $^{14}\text{N}$  hyperfine couplings because of their known nuclear  $g$  values. The final details of a precise parameter determination, including second-order effects, will have to come from a single-crystal study.

**B. Carp Hemoglobin Azides.** The spectra observed from the carp hemoglobins are similar to those seen from human hemoglobin, although we do note differences in the 4–5-MHz region at  $g_x$  (Figure 7a vs. 8). The simple conclusion from a comparison of the high- and low-pH nitrogen ENDOR spectra of Figure 8 is that there is little concomitant change of the ENDOR spectra, which we have assigned to heme nitrogen, with the R to T transition known to occur as a function of pH in fish hemoglobins. The change in electronic  $g$  values of fish hemoglobins on going from high- to low-pH forms has been interpreted to show a change in the strength of the axial perturbation upon going from R to T forms.<sup>6</sup> Such a change points to a change in the strength of the bond with the *axial* ligands rather than with the heme nitrogens. Thus, we believe that we should direct future work toward comparing ENDOR from axial ligands of hemoglobins undergoing conformational change.

**Results. Nitrogen ENDOR from Methemoglobin and Metmyoglobin Cyanides.** We had previously reported ENDOR from metmyoglobin cyanide but had not assigned it to heme

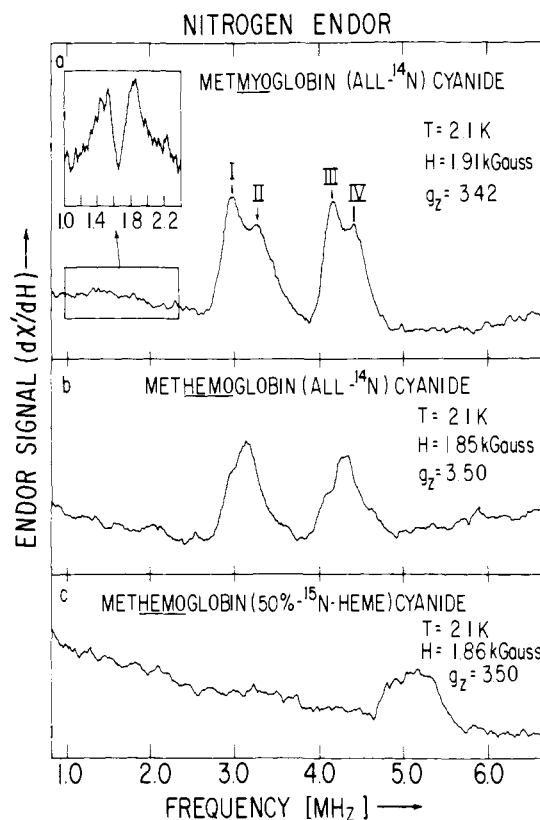


**Figure 9.** Nitrogen ENDOR from the nitrogen of cyanide derivatives of all- $^{14}\text{N}$  metmyoglobin and hemoglobin and of methemoglobin containing 50%  $^{15}\text{N}$  on the heme. The first two samples were about 5 mM in heme while the last was about 1 mM. In (a) the lines labeled I, II, III, and IV are respectively at 2.90, 3.19, 4.11, and 4.34 MHz (all  $\pm 0.03$  MHz). The spectra each required about 1 h of signal averaging.

or to histidine nitrogens.<sup>3f</sup> We found pairs of intense peaks in the 2.5–4.5-MHz region, shown in Figure 9a, and the splitting of these peaks was close to the appropriate Zeeman splitting for nitrogens. There were also some weaker lines in the 1–2-MHz region noted in ref 3f, and we show these in more detail in the inset to Figure 9a. In Figure 9b we show nitrogen ENDOR from methemoglobin cyanide with spectral features in the same general region as from metmyoglobin cyanide, although the signal to noise is somewhat poorer than for the myoglobin. In the sample of hemoglobin that was enriched to 50% in  $^{15}\text{N}$  on the heme we saw (Figure 9c) a decrease in intensity of the peaks in the 2.5–4.5-MHz region and the appearance of a new ENDOR peak near 5.1 MHz. No other lines were seen above 5 MHz. With signal averaging over a narrower frequency range than in Figure 9c a weak peak appeared near 3.25 MHz which might be the  $^{15}\text{N}$  Zeeman partner to the peak near 5 MHz. Although the  $^{15}\text{N}$  sample was quite dilute and its signal weak, a comparison of its signal to that of all- $^{14}\text{N}$  hemoglobin and myoglobin is adequate to prove that the more intense peaks in the 2.5–4.5-MHz region of all- $^{14}\text{N}$  hemoglobin and myoglobin must be from *heme* nitrogens. For the sake of completeness we also looked at metmyoglobin prepared with  $\text{C}^{15}\text{N}^-$  and found two very weak resonances appearing near 1.80 and 3.45 ( $\pm 0.06$ ) MHz. The intensity of the four previously observed strong resonances in the 2.5–4.5-MHz region did not change with use of  $\text{C}^{15}\text{N}^-$ .

**Theory and Discussion. Nitrogen ENDOR of Methemoglobin and Metmyoglobin Cyanides.** We considered in our previous analysis of the metmyoglobin cyanide data that the four intense lines in the 2.5–4.5-MHz region were simply a single four-line multiplet from one type of nitrogen.<sup>3f</sup> These are the four lines marked I, II, III, and IV in Figure 9a, whose frequencies are

given in its figure legend. The resultant preliminary analysis gave  $|^{14}A_{zz}| = 7.15$  MHz and  $|P_{zz}| = 0.15$  MHz.<sup>3f</sup> However, if the weaker peaks in the 1–2-MHz region are really Zeeman partners of the stronger peaks in the 2.5–4.5-MHz region and if  $|P_{zz}| \approx |^{14}g_N\beta_n H|$  (as was approximately the case with the heme nitrogens in the azide compounds), then there will be a somewhat different interpretation with different couplings for two inequivalent types of heme nitrogen. For example, a choice of I, III, or II, IV as separate partners to fit the ENDOR frequency expressions (6a-1) and (6a-2) yields  $|^{14}A_{zz}| = 5.84$ ,  $|P_{zz}| = 0.60$  for I, III and  $|^{14}A_{zz}| = 6.36$ ,  $|P_{zz}| = 0.58$  for II, IV. Because of the poorer experimental resolution of the low-frequency ENDOR peaks in the 1–2-MHz range in Figure 9a, we must consider this newer interpretation less definite than the interpretation at  $g_z$  of the corresponding azide data. As an additional check on the value of the heme nitrogen hyperfine coupling, we took the  $^{15}\text{N}$  peak at 5.1 MHz as the higher frequency member of the  $^{15}\text{N}$  Zeeman pair (eq 6b), computed a  $^{15}\text{N}$  hyperfine coupling of 8.6 MHz from it, and then back-calculated a  $^{14}\text{N}$  hyperfine coupling of about 6.1 MHz.

We have noted the recent NMR results on  $\text{C}^{15}\text{N}^-$  metmyoglobin in ref 26, where a downfield shift of 950 ppm was reported. We compute from this NMR data an expected contact interaction of +3.7 MHz. Our own  $\text{C}^{15}\text{N}^-$  ENDOR data yield a net  $^{15}\text{N}$  hyperfine coupling of about 5.25 MHz.

**Acknowledgments.** We are grateful to Professor Y. P. Myer of the Chemistry Department, SUNY at Albany, in whose laboratory many of the hemoglobin and myoglobin preparations were carried out. We thank Professors J. C. W. Chien, B. M. Hoffman, and Q. H. Gibson for very useful discussions on the properties of carp hemoglobins. Dr. Edwin Taft of the Albany Medical Center Hospital provided facilities for hemoglobin collection. This work was supported by NIH Grant AM 17884 and NIH Biomedical Institutional Grant 5 SO7 RR 07122. C. P. Scholes is the recipient of NIH Research Career Development Award 1 KO4 AM00274.

**Supplementary Material Available:** An appendix that includes one figure (S1) and (a) gives a theoretical explanation for the expected electronic inequivalence of heme nitrogens in low-spin ferric hemes. (b) discusses a more general heme nitrogen spin Hamiltonian than that used in the text. (c) estimates the  $^{14}\text{N}$  hyperfine parameters at  $g_x$  in hemoglobin azide; also a table (I-S) that gives a more complete set of proton hyperfine couplings for the aquo, fluoro, and cyanide derivatives of myoglobin and hemoglobin (10 pages). Ordering information is given on any current masthead page.

## References and Notes

- (1) (a) State University of New York at Albany; (b) University of Massachusetts; (c) Weizmann Institute of Science.
- (2) This work was taken from the thesis of C. F. Mulks, submitted in partial fulfillment of the requirements for Ph.D. at the State University of New York at Albany.
- (3) (a) C. P. Scholes, R. A. Isaacson, and G. Feher, *Biochim. Biophys. Acta*, **263**, 448–452 (1972); (b) C. P. Scholes, R. A. Isaacson, T. Yonetani, and G. Feher, *ibid.*, **322**, 457–462 (1973); (c) G. Feher, R. A. Isaacson, C. P. Scholes, and R. L. Nagel, *Ann. N.Y. Acad. Sci.*, **222**, 86–101 (1973); (d) H. L. Van Camp, C. P. Scholes, and C. F. Mulks, *J. Am. Chem. Soc.*, **98**, 4094–4098 (1976); (e) H. L. Van Camp, C. P. Scholes, C. F. Mulks, and W. S. Caughey, *ibid.*, **99**, 8283–8290 (1977); (f) C. P. Scholes and H. L. Van Camp, *Biochim. Biophys. Acta*, **434**, 290–296 (1976).
- (4) M. K. Mallick, J. C. Chang, and T. P. Das, *J. Chem. Phys.*, **68**, 1462–1473 (1978).
- (5) (a) R. W. Noble, L. S. Parkhurst, and Q. H. Gibson, *J. Biol. Chem.*, **245**, 6628–6633 (1970); (b) R. R. Pennelly, A. L. Tan-Wilson, and R. W. Noble, *ibid.*, **250**, 7239–7244 (1975).
- (6) L. C. Dickinson and J. C. W. Chien, *J. Biol. Chem.*, **252**, 1327–1330 (1977).
- (7) H. L. Van Camp, C. P. Scholes, and R. A. Isaacson, *Rev. Sci. Instrum.*, **47**, 516–517 (1976).
- (8) D. L. Drabkin, *J. Biol. Chem.*, **164**, 703–723 (1946). See p 705.
- (9) A. Lapidot and C. S. Irving, *Proc. Int. Conf. Stable Isot.*, **2nd**, 427–444 (1975).
- (10) N. C. Watson, *Prog. Stereochem.*, **4**, 299–333 (1969).
- (11) In calculating distances and angles to CH or NH protons, we took the CH or NH bond lengths as being 1 Å along the bisector of the appropriate bond angle centered at a C or N.
- (12) L. Pauling, "Nature of the Chemical Bond", 3rd ed., Cornell University Press, Ithaca, N.Y., 1960; bond angle, p 111; bond length, p 466.
- (13) In our calculations we have also used the more recent metmyoglobin coordinates of Takano, and for the protons discussed here have found similar results to those calculated using the coordinates of ref 10. However, the Takano coordinates indicate that one of the oxygens of a heme propionic acid curls back toward the heme, and, if we were to consider an exchangeable proton to be bonded to this oxygen, we compute a dipolar interaction for this proton of about 0.7 MHz. T. Takano, *J. Mol. Biol.*, **110**, 537–568 (1977).
- (14) Preliminary measurements on the nitrogens of fluorometmyoglobin were done in Feher's laboratory in 1972–1973.
- (15) In frozen solutions of metmyoglobin and hemoglobin, prepared without glycerol but with excess diamagnetic CO protein, we were able to obtain ENDOR from  $^{13}\text{CN}^-$  ligand. The resulting hyperfine couplings for the cyanide differ slightly from the case where glycerol was present, giving  $|A_{zz}| = 27.9$  MHz for myoglobin and  $|A_{zz}| = 27.3$  MHz for hemoglobin.
- (16) H. Goff, *J. Am. Chem. Soc.*, **99**, 7723–7724 (1977).
- (17) A. Lowenstein, M. Shporer, and G. Navon, *J. Am. Chem. Soc.*, **85**, 2855–2856 (1963).
- (18) D. G. Davis and R. G. Kurland, *J. Chem. Phys.*, **46**, 388–389 (1967).
- (19) H. A. Kuska and M. T. Rogers, *J. Chem. Phys.*, **41**, 3802–3808 (1964).
- (20) R. G. Shulman, S. H. Glarum, and M. Karplus, *J. Mol. Biol.*, **57**, 93–115 (1971).
- (21) We have not yet looked at ENDOR from cyanide derivatives of ferric porphyrin model compounds that lack meso protons. Thus, our assignment of meso protons in the cyanide compounds cannot yet be considered as experimentally definitive as the assignment of meso protons in the high-spin hemes where we saw no meso proton ENDOR from tetraphenylporphyrins that lacked meso protons.
- (22) J. S. Frye and G. N. La Mar, *J. Am. Chem. Soc.*, **97**, 3561–3562 (1975).
- (23) We have found as a general experimental fact that the Zeeman-related pairs of ENDOR lines for both  $^{14}\text{N}$  and  $^{15}\text{N}$  in heme systems appear with the higher frequency member of each pair the more intense. We have previously seen this for high-spin ferric heme nitrogens,<sup>3a-e</sup> and it also appears to be the case for low-spin ferric hemes. Intensity differences in the ENDOR from a particular nucleus can happen because of the competing effects on ENDOR transition probability from direct ENDOR-induced nuclear transitions and from ENDOR-induced modulation of the hyperfine coupling. A. Abragam and B. Bleaney, "Electron Paramagnetic Resonance of Transition Ions", Oxford University Press, London, 1970, Section 4.3.
- (24) G. A. Helcké, D. J. E. Ingram, and E. F. Slade, *Proc. R. Soc. London, Ser. B*, **169**, 275–288 (1968).
- (25) Nuclear  $g$  factors for  $^{14}\text{N}$  and  $^{15}\text{N}$  are respectively 0.404 and  $-0.566$ .
- (26) I. Morishima and T. Inubishi, *J. Am. Chem. Soc.*, **100**, 3568–3574 (1978).